

Spectral function of a hole in a Hubbard antiferromagnet

S. A. Trugman

Theoretical Division, Los Alamos National Laboratory, Los Alamos, New Mexico 87545

(Received 5 July 1989; revised manuscript received 20 October 1989)

The Green's function $G(\mathbf{k}, \omega)$ is calculated for a hole in a Hubbard antiferromagnet by a new nonperturbative, variational method for an infinite square lattice. The quasiparticle and excited-state wave functions show that the substantial structure in the "incoherent" spectrum is related to string states for large U . The strength of the quasiparticle pole and the anisotropic effective mass are obtained as a function of (U/t) . The quasiparticle lifetime is infinite for most \mathbf{k} .

There has been renewed interest in the dynamics of holes in the Mott-Hubbard insulating state, in part because holes are the charge carriers in the high-temperature superconducting oxides. A hole in an antiferromagnetic Mott insulator can only move in first order by emitting or absorbing a spin wave.¹ This makes the problem more difficult than that of interacting electrons and phonons, which has a simple limit in which the electrons and phonons decouple.

The Green's function $G(\mathbf{k}, \omega)$ is calculated. It contains information about both ground and excited states at any given momentum \mathbf{k} . Several studies have considered the ground-state properties of one or more holes in the Hubbard quantum antiferromagnet.²⁻⁵ Others have calculated the density of states, which is the imaginary part of $G(\mathbf{k}, \omega)$ averaged over all \mathbf{k} .^{6,7} Kane, Lee, and Read have calculated the spectral function [imaginary part of

$G(\mathbf{k}, \omega)$] by diagrammatic perturbation theory, and find a featureless incoherent spectrum above a quasiparticle pole⁸ (see also Ref. 9). In one dimension, however, some calculations show more structure.¹⁰

The one-band Hubbard model on a square lattice is used to model the CuO_2 planes of the oxide superconductors. It has a Mott insulating state for one electron per site. The Hubbard Hamiltonian is

$$H_H = -t \sum_{\langle j,k \rangle, s} (c_{j,s}^\dagger c_{k,s} + \text{H.c.}) + U \sum_j n_{j,\uparrow} n_{j,\downarrow}. \quad (1)$$

For moderate or large U , the Hubbard Hamiltonian can be transformed into an effective Hamiltonian by removing the doubly occupied sites using second-order perturbation theory.¹¹ The transformed Hamiltonian is $H = PH_1P$, where P is the projection operator onto the subspace with no doubly occupied sites, and

$$H_1 = -t \sum_{\langle j,k \rangle, s} (c_{j,s}^\dagger c_{k,s} + \text{H.c.}) + J \sum_{\langle j,k \rangle} (\sigma_j \cdot \sigma_k - n_j n_k) - t' \sum_{\langle j,k,m \rangle, s} (c_{j,s}^\dagger n_{k,-s} c_{m,s} + \text{H.c.}) + t' \sum_{\langle j,k,m \rangle, s} (c_{j,-s}^\dagger c_{k,s}^\dagger c_{k,-s} c_{m,s} + \text{H.c.}). \quad (2)$$

Both J and t' are equal to t^2/U and $\langle j,k,m \rangle$ and three distinct adjacent sites. The hopping parameter $t=1$ in the remainder of this paper. The t' terms cause a hole to hop to a next-nearest-neighbor site. The J term describes a Heisenberg antiferromagnet, and is the only operative term at half-filling (one electron per site). The ground state at half-filling is a Néel antiferromagnet with spin-wave fluctuations.¹² This motivates writing $\sigma_j \cdot \sigma_k = \sigma_j^+ \sigma_k^- + 2(\sigma_j^+ \sigma_k^- + \sigma_j^- \sigma_k^+)$, and treating the last term perturbatively (to infinite order). In contrast to the $t-t'-J$ model considered here, some authors have investigated the simpler $t-J$ model, in which the last two $O(t^2/U)$ terms in Eq. (2) are omitted. The $t-J$ approximation gives a substantially smaller quasiparticle bandwidth for $U \lesssim 10$; compare Trugman³ and Sachdev.⁵

The calculation defines a variational Hilbert space for an infinite lattice, and exactly solves for the Green's function of the Hamiltonian (2) in the variational space without further approximation. A similar method was first used in Ref. 3 for ground-state properties. The variational space is defined as follows: The first states included have the hole occupying any lattice position, with the spins

in the unperturbed (Ising) Néel state. There are N such states, where the number of sites in the lattice $N = \infty$. For each hole position, states are added with various numbers of spin flips (with respect to the Néel state) in the vicinity of the hole. The number of states in the Hilbert space is NM , where M is the number of spin configurations retained per hole location. As explained in Ref. 3, the matrix elements of this many-body problem are identical to those of a one-body tight-binding problem for a single particle. The sites of the tight-binding problem do not, however, represent Wannier states, but rather many-body configurations. The tight-binding model forms an infinite periodic lattice, with M sites per unit cell. Each exact eigenstate has a Bloch wave vector \mathbf{k} . The Bloch symmetry reduces the intractable numerical problem of diagonalizing an $NM \times NM$ matrix, with $N = \infty$, to that of diagonalizing an $M \times M$ matrix for fixed \mathbf{k} .

This infinite lattice calculation allows properties to be obtained at any wave vector \mathbf{k} , and not just at a small set of allowed vectors in a small system diagonalization. It is not equivalent to a small system calculation, even one in which the allowed \mathbf{k} are shifted by boundary conditions.

Even a single hole in a small system introduces a finite-hole density because of its periodic images.

The calculations below are for a variational Hilbert space with 609 states per lattice site. (The issue of adequate size for the Hilbert space is addressed at the end.) The variational space respects all lattice symmetries. This space contains up to five spin flips, with a maximum distance of five between the hole and a spin flip. The Hilbert space is generated by repeatedly acting on the reference state (a hole at the origin with spins in the Néel configuration) by the t and t' off-diagonal terms in the Hamiltonian (2). All translations are also included. Let "1" represent a t hop and "2" a t' hop. The sequence (1) hops a hole to a nearest-neighbor site, leaving an overturned spin. Any state obtained from the reference state by a sequence whose elements add up to four or less is included in the variational space. In addition, five sequences that add to five are included: (2111), (221), (212), (1111), and (1112). The last represents the set of states that can be obtained from the reference state by acting first with three t hops, and then with either of the t' hops. The algorithm does not double count basis states. The real-space basis takes account of facts that are subtle in momentum space, such as the fact that s_z of an up spin can be lowered once, but not twice. The calculation includes hole propagation by moving two steps and having the overturned spins restored by the $\sigma^+\sigma^-$ term or the conjugate process where the vacuum fluctuation occurs first, propagation by traversing a plaquette $1\frac{1}{2}$ times without a spin flip, and by many more complicated processes.³

The Green's function is

$$G(\mathbf{k}, \omega) = \sum_j \left[\frac{|\langle j | c_{\mathbf{k}}^\dagger | 0 \rangle|^2}{\omega - (E_j - E_0) + i\eta} + \frac{|\langle j | c_{\mathbf{k}} | 0 \rangle|^2}{\omega + (E_j - E_0) - i\eta} \right], \quad (3)$$

where $c_{\mathbf{k}}^\dagger$ is the creation operator for holes of a definite spin (up), $|0\rangle$ is the Mott-insulator (Néel) state, and $|j\rangle$ is a complete set of states. $G(\mathbf{k}, \omega)$ for holes is calculated directly from the first term of Eq. (3) by inserting the eigenstates for the variational space. The spectral function $A(\mathbf{k}, \omega)$ is the imaginary part of $G(\mathbf{k}, \omega)$. (The real part may be recovered by Kramers-Kronig.) The spectral function for fixed \mathbf{k} is represented in this approximation as a sum of a finite number of δ functions (609 in this case) with varying weight. If the true spectral function contains a continuum part, the approximation represents it as a large number of closely spaced δ functions, each with small weight.

Figure 1(a) is the spectral function for $U=8$, $\mathbf{k}=(\pi/2, \pi/2)$. The quasiparticle energy is a minimum at this wave vector, denoted "X." There is a large quasiparticle pole labeled (1) at energy -2.529 , which contains a fraction $Z=0.358$ of the total spectral weight. The "continuum" at higher energy has a good deal of structure. There is, for example, a substantial second peak (2) at energy -0.259 with weight 0.175.

For large U , some peaks can be interpreted in terms of an approximate linear confining potential or string description of the model.^{2,4,6} It assumes that the Hilbert

space is a Bethe lattice with energy that depends only on the distance from the origin. (The fact that the structure is not quite a Bethe lattice and that some states have much less energy³ is neglected in this approximation.)

The eigenfunctions are compared to those for the string approximation. The string eigenstates are obtained by diagonalizing a Bethe lattice with six levels. (The variational space of 609 states contains six levels of the Bethe lattice, as well as states that are not represented by a Bethe lattice, such as those generated by t' , in which the spins and hole are not contiguous.) For $U=20$, the six string eigenstates can all be identified with major peaks in the spectral function [Fig. 1(b)]. The string energies differ by less than 0.38 from the corresponding variational energies. Direct comparison of the wave functions, however, is a more sensitive test. The quantity r is defined as the normalized overlap between a variational eigenfunction and a string eigenfunction on the first four levels of the Bethe lattice: $r = \mathbf{v}_i \cdot \mathbf{w}_j / |\mathbf{w}_j|^2$, where \mathbf{v}_i is a variational eigenstate and \mathbf{w}_j is a string eigenstate, each restricted to the first four levels. The overlap $r=0.944$ for the quasiparticle (lowest energy) eigenstate and the lowest-energy string state. Although the string eigenstate has equal amplitudes for all basis states at the same level of the Bethe lattice, the quasiparticle eigenstate does not. This symmetry is broken at the third and higher levels of the Bethe lattice. The amplitudes range from 0.177 to 0.090 at the third level and from 0.088 to 0 at the fourth level. The radially excited string states 2 through 6 have a smaller overlap of 0.6 to 0.7 with states corresponding to peaks in the spectral function.

As U decreases, it becomes more difficult to identify major spectral peaks with string states. At $U=8$, the quasiparticle eigenfunction has an overlap $r=0.877$ with the lowest string eigenstate. The equivalence of states at the same Bethe lattice level is broken even more strongly at $U=8$. The second peak, (2) in Fig. 1(a), has overlap $r=0.693$ with the first excited string state. It has not proven possible to assign the other large amplitude peaks to string states. Many eigenstates have substantial probability not to be on the Bethe lattice at all (t' states). In the intermediate and large- U regime where the string model is useful, it is *not* correct to identify a major spectral peak as having a fixed number of spin waves. The eigenstates are coherent superpositions of states with zero, one, . . . , spin flips, with the energy determined primarily by the phase of the superposition.

In the limit $J \gg t$, the $t-t'-J$ model considered here has little to do with the Hubbard model, because the neglect of higher-order terms in U^{-1} in the Hamiltonian can no longer be justified. (This is even more true of the $t-J$ model.) The spectral function has a width of $O(t)$ for $U \gg t$ and $O(J)$ for $U \ll t$. The high-energy portion of the spectral function has a low weight, however, for large J [see Fig. 1(d)].

The effective mass of the quasiparticle can be calculated from the energy of the quasiparticle pole as a function of \mathbf{k} . As measured by the bandwidth [difference between the lowest-energy states at $\mathbf{k}=(0,0)$ and at X], the effective mass at $U=8$ is $m=5.92$, in units where the effective mass of a single electron on the same lattice is

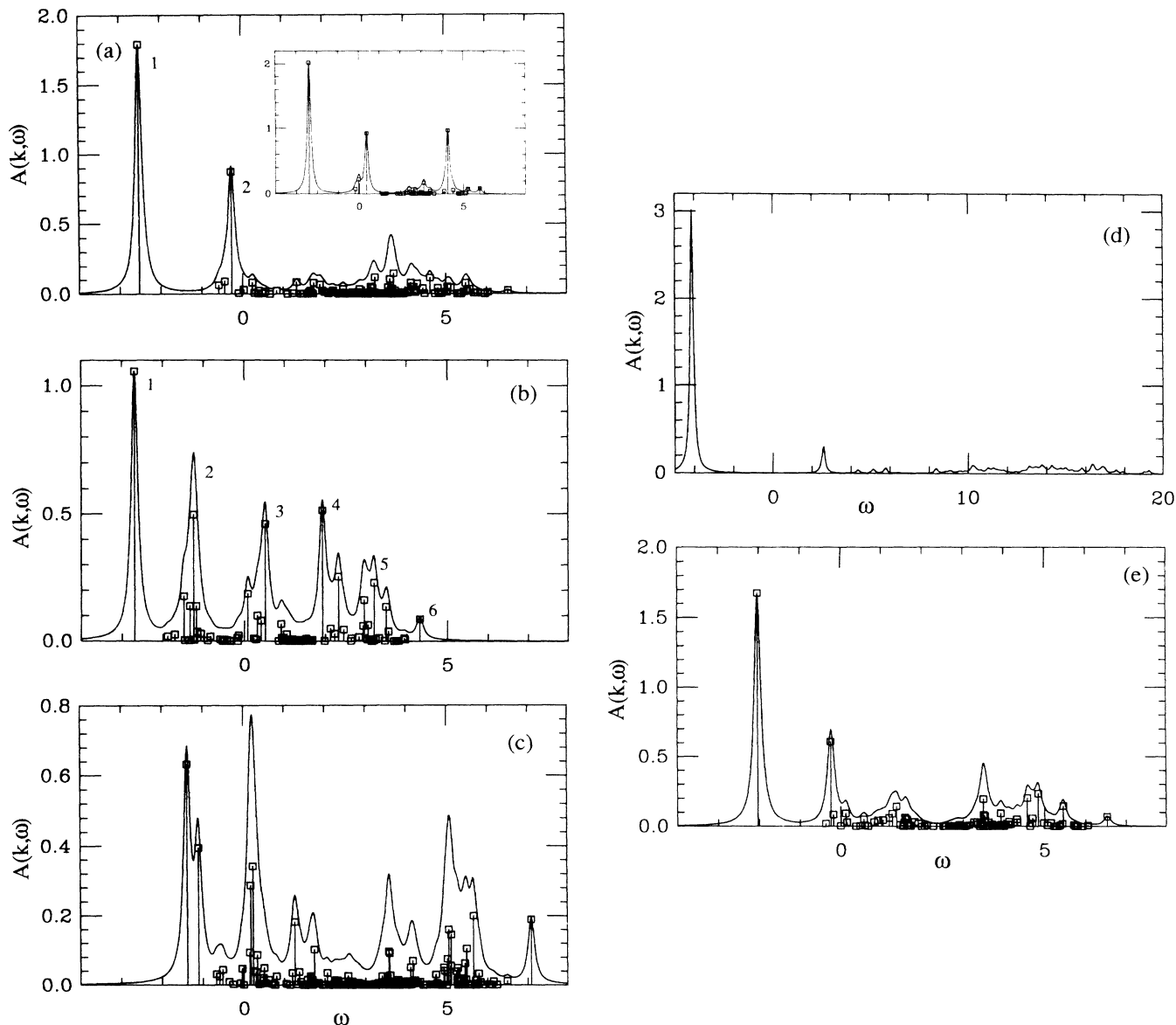


FIG. 1. The spectral function $A(\mathbf{k}, \omega)$ plotted vs ω . A δ function generated in this approximation is given by a vertical line with a square on top, of height proportional to the amplitude. The smooth spectral function is obtained by giving each δ function a width $\eta=0.1$. All plots except the inset use a variational space of 609 states per lattice site. (a) $U=8$, $\mathbf{k}=X=(0.5\pi, 0.5\pi)$; inset: 197 states. (b) $U=20$, $\mathbf{k}=X$. (c) $U=8$, $\mathbf{k}=(0.15\pi, 0.15\pi)$. (d) $U=2$, $\mathbf{k}=X$, δ functions omitted. (e) Spectral function for the t - J model, same parameters as (a). All figures but (d) have the same horizontal scale.

one. (The effective mass is not greatly changed from that calculated with a much smaller variational basis of size 49, which gives $m=5.47$; see Ref. 3.) The effective mass can also be defined by the curvature of the quasiparticle energy $\partial^2 E(\mathbf{k})/\partial k_\alpha \partial k_\beta$ at X , compared with the curvature of a free electron at its band minimum ($\mathbf{k}=0$). This definition results in a highly anisotropic mass, $m=(1.28, 34.91)$, where the first number is in the (1,1) direction and the second in the (1, -1) direction. For $U=20$ the effective mass is $m=14.73$ from the bandwidth, and $m=(3.58, 30.79)$ from the curvature. For $U \leq 30$, the bandwidth W is well fit by a power law in $J=1/U$. The best fit is essentially linear, $W=aJ^\alpha$, with $a=13.04$ and $\alpha=1.07$. For the t - t' - J model, this fit continues to be

good down to the smallest U investigated ($U=0.5$). This result is in agreement with the t - J calculations of Kane, Lee, and Read,⁸ but differs from Ref. 16, which obtains a bandwidth that scales as $J^{2/3}$ (see also Ref. 9).

It is of interest to know whether the exact quasiparticle pole has an intrinsic width (intrinsic imaginary part) for $\eta \rightarrow 0$. For a very large basis set, the approximation used represents a pole with an intrinsic imaginary part as a closely spaced group of δ functions, and a pole with no imaginary part as a single δ function. For \mathbf{k} just off the point X , the closest δ function to the quasiparticle pole for $U=8$ is a substantial energy 1.053 away. This is to be contrasted with pole (2), Fig. 1(a), whose nearest δ function is only 0.015 away. The evidence suggests that the

intrinsic width of the quasiparticle is zero near the point X , but that the second pole has a nonzero intrinsic width.

Moving from X toward $\mathbf{k}=\mathbf{0}$, the δ functions move closer to the quasiparticle pole, but the nearest is still 0.683 away at $\mathbf{k}=(0.3\pi, 0.3\pi)$. The quasiparticle appears to have an infinite lifetime even a substantial distance from X . This may be explained by the fact that a moving quasiparticle cannot radiate spin waves while conserving energy and momentum unless its group velocity exceeds the spin-wave velocity, in which case it Cherenkov radiates spin waves.⁸ Since the quasiparticle bandwidth is $O(J)$ due to many-body interactions, \mathbf{k} must move substantially away from X to have a chance to Cherenkov radiate. As \mathbf{k} approaches the origin, the closest δ function approaches arbitrarily near to the quasiparticle pole as $|k|^2$. The strength of the quasiparticle pole Z vanishes as \mathbf{k} approaches the origin, also as $|k|^2$; see Fig. 1(c). At $\mathbf{k}=\mathbf{0}$, the lowest-energy state is doubly degenerate, with the symmetry of a p orbital and zero spectral weight.

The spectral weight Z in the quasiparticle pole at X decreases as U increases. As U increases in the sequence (2, 4, 8, 20, 40), Z decreases as (0.603, 0.504, 0.358, 0.211, 0.152). In the interval $4 \leq U \leq 40$, Z is well fit by a power law. The best fit is approximately a square root, $Z=bJ^\beta$, with $b=1.063$ and $\beta=0.532$. This is to be contrasted with Ref. 8 which obtains $\beta=1$ and Ref. 4 which contains $\beta=1$ in the Ising limit. See also Ref. 9.

We now address the question of whether the variational space is large enough to obtain a reliable spectral function. Figure 1(a), inset, is the $U=8$ spectral function with a variational space about $\frac{1}{3}$ the size of the others (197 states). In going from the smaller to larger calculation, the quasiparticle amplitude and energy shift from (0.404, -2.394) to (0.358, -2.529). The second peak shifts from (0.185, 0.351) to (0.175, -0.259). Both calculations show spectral weight at higher energy, although the large calculation spreads the weight more evenly. The spectral function converges first at lower energies. This

suggests that the spectral function is unlikely to be substantially altered at low energies by using a variational space even larger than 609 states, but that some shifting of weight and perhaps smoothing may occur at higher energies. The range of validity of the scaling laws indicates that for $U > 30$, a larger Hilbert space is required.

The spectral function has also been calculated for the t - J model, as opposed to the t - t' - J model considered above. The calculation shown in Fig. 1(e) is for the same 609 state variational space, with a modified Hamiltonian that omits the two t' terms in the Hamiltonian, Eq. (2). The t - J Hamiltonian causes the quasiparticle peak to shift to higher energy (and to have a different dispersion as a function of \mathbf{k}). The spectral weight above the second pole is distributed differently for the t - J model.

An increased quasiparticle effective mass due to many-body effects is observed experimentally.^{13,14} The structure in the spectral function, caused by strong coupling between holes and spin waves, should in principle be observable in tunneling and photoemission experiments. This method is applicable to a broad class of problems, including the polaron problem.¹⁵

After this research was completed, I learned that Dagotto *et al.* were calculating the spectral function of the t - J model by a different technique on a 4×4 lattice.¹⁶ The agreement is fairly good, and improves if comparison is made with the t - J rather than the t - t' - J results. See Ref. 17 for other recent results on small-system spectral functions.

I would like to thank S. Girvin, K. Bedell, E. Dagotto, B. Halperin, M. Johnson, A. Kampf, R. Silver, and F. Zhang for useful discussions. This work was supported by the Department of Energy, and by the Institute for Theoretical Physics at Santa Barbara through National Science Foundation Grant No. PHY82-17853 and a grant from NASA.

¹E. L. Nagaev, Zh. Eksp. Teor. Fiz. **58**, 1269 (1970) [Sov. Phys. JETP **31**, 682 (1970)].

²L. N. Bulaevskii, E. L. Nagaev, and D. I. Khomskii, Zh. Eksp. Teor. Fiz. **54**, 1562 (1968) [Sov. Phys. JETP **27**, 836 (1968)].

³S. A. Trugman, Phys. Rev. B **37**, 1597 (1988).

⁴B. I. Shraiman and E. D. Siggia, Phys. Rev. Lett. **60**, 740 (1988).

⁵J. R. Schrieffer, X. G. Wen, and S. C. Zhang, Phys. Rev. Lett. **60**, 944 (1988); S. Sachdev, Phys. Rev. B **39**, 12232 (1989); J. A. Riera and A. P. Young, *ibid.* **39**, 9697 (1989); E. Dagotto, A. Moreo, and T. Barnes, *ibid.* **40**, 6721 (1989); J. Bonca, P. Prelovsek, and I. Sega, *ibid.* **39**, 7074 (1989); W. Bauer and S. E. Koonin, *ibid.* **38**, 8958 (1988); Z. B. Su, Y. M. Li, W. Y. Lai, and L. Yu, Phys. Rev. Lett. **63**, 1318 (1989); Y. Hasegawa and D. Poilblanc, Phys. Rev. B **40**, 9035 (1989).

⁶W. F. Brinkman and T. M. Rice, Phys. Rev. B **2**, 1324 (1970).

⁷R. Joynt, Phys. Rev. B **37**, 7979 (1988); H. Tsunetsugu and Y. Takahashi (unpublished).

⁸C. Kane, P. Lee, and N. Read, Phys. Rev. B **39**, 6880 (1989).

⁹C. Gros and M. D. Johnson, Phys. Rev. B **40**, 9423 (1989).

¹⁰S. Schmitt-Rink, C. Varma, and A. Ruckenstein, Phys. Rev. Lett. **60**, 2793 (1988).

¹¹A. B. Harris and R. V. Lange, Phys. Rev. **157**, 295 (1967).

¹²J. D. Reger and A. P. Young, Phys. Rev. B **37**, 5978 (1988).

¹³G. A. Thomas *et al.*, Phys. Rev. Lett. **61**, 1313 (1988).

¹⁴D. Reagor, E. Ahrens, S.-W. Cheong, A. Migliori, and Z. Fisk, Phys. Rev. Lett. **62**, 2048 (1989).

¹⁵S. A. Trugman (unpublished); I. Batistic, S. Marianer, and S. A. Trugman (unpublished).

¹⁶E. Dagotto, A. Moreo, R. Joynt, S. Bacci, and E. Gagliano (unpublished).

¹⁷K. von Szczepanski, P. Horsch, W. Stephan, and M. Ziegler (unpublished); C.-X. Chen, H.-B. Schuttler, and A. J. Fedro (unpublished); I. Sega and P. Prelovsek (unpublished); H. J. Schmidt and Y. Kuramoto (unpublished).